

PAPER

Comparison of the Green–Kubo and homogeneous non-equilibrium molecular dynamics methods for calculating thermal conductivity

To cite this article: B Dongre *et al* 2017 *Modelling Simul. Mater. Sci. Eng.* **25** 054001

View the [article online](#) for updates and enhancements.

Related content

- [Effect of lattice relaxation on thermal conductivity of fcc-based structures: an efficient procedure of molecular dynamics simulation](#)
Min Young Ha, Garam Choi, Dong Hyun Kim *et al.*
- [Atomistic study of the influence of lattice defects on the thermal conductivity of silicon](#)
T Wang, G K H Madsen and A Hartmaier
- [Heat conduction in one-dimensional oscillator lattices using Nose–Hoover chain thermostats](#)
M Romero-Bastida and J F Aguilar

Comparison of the Green–Kubo and homogeneous non-equilibrium molecular dynamics methods for calculating thermal conductivity

B Dongre¹, T Wang² and G K H Madsen¹

¹Institute of Materials Chemistry, TU Wien, A-1060 Vienna, Austria

²Atomistic Modelling and Simulation, Interdisciplinary Centre for Advanced Materials Simulation (ICAMS), Ruhr-University Bochum, Germany

E-mail: georg.madsen@tuwien.ac.at

Received 24 January 2017, revised 20 April 2017

Accepted for publication 25 April 2017

Published 15 May 2017



CrossMark

Abstract

Different molecular dynamics methods like the direct method, the Green–Kubo (GK) method and homogeneous non-equilibrium molecular dynamics (HNEMD) method have been widely used to calculate lattice thermal conductivity (κ_ℓ). While the first two methods have been used and compared quite extensively, there is a lack of comparison of these methods with the HNEMD method. Focusing on the underlying computational parameters, we present a detailed comparison of the GK and HNEMD methods for both bulk and vacancy Si using the Stillinger–Weber potential. For the bulk calculations, we find both methods to perform well and yield κ_ℓ within acceptable uncertainties. In case of the vacancy calculations, HNEMD method has a slight advantage over the GK method as it becomes computationally cheaper for lower κ_ℓ values. This study could promote the application of HNEMD method in κ_ℓ calculations involving other lattice defects like nanovoids, dislocations, interfaces.

Keywords: Green–Kubo, HNEMD, Stillinger–Weber, thermal conductivity, vacancies

(Some figures may appear in colour only in the online journal)

1. Introduction

Due to miniaturization of devices, increasing thermal loads and higher efficiency demands there is an ever-growing demand for materials with tailored thermal conductivities (κ) [1]. On one hand, devices like high power semiconductor electronic devices and lasers require high κ

for efficient heat removal which is critical to their performance. On the other hand, very low κ is required in thermoelectric devices whose performance is inversely proportional to κ .

In semiconductors and insulators κ is dominated by the lattice part κ_ℓ . Classical molecular dynamics (MDs) simulations are a powerful tool for calculating κ_ℓ due to their atomic resolution that helps to understand the underlying mechanisms leading to a specific κ_ℓ . The conceptually simplest MD method for calculating κ_ℓ is the direct method [2–6] where a temperature gradient is applied over a simulation box and the thermal conductivity is extracted from Fourier’s law. However, the temperature gradients that must be applied are orders of magnitude larger than in experiments. Furthermore, the long mean free paths of the low frequency phonons make it difficult to converge the results [7].

An alternate MD method for calculating κ_ℓ is the Green–Kubo (GK) method [8]. The GK method applies linear response theory to the fluctuations of the heat current in a homogeneous equilibrium system. It requires integration of the auto-correlation function, which makes the method numerically challenging to apply. Another technique called homogeneous non-equilibrium molecular dynamics (HNEMD) circumvents the calculation of the auto-correlation function. The HNEMD method was initially proposed by Evans to calculate κ_ℓ [9], who applied it to systems with pairwise interactions. The technique was subsequently applied to study systems with higher-order interactions among the particles [10–12].

To design materials with desired thermal conductivities, understanding the effects of defects is of prime importance. Defects like vacancies, dislocations, interfaces etc are inevitably present in materials of technological interest. Such defects break the symmetry of the crystal structures and scatter the phonons thereby affecting the energy transported by phonons in solids. Vacancies in particular are very important because of their high concentrations at elevated temperatures. They act both as a large mass perturbation and perturb the bonding in the lattice and therefore strongly effect κ_ℓ [13–16].

There has not been a systematic comparison of HNEMD with other methods in literature. In this work we fill this gap by doing a systematic comparison of the GK and HNEMD methods in terms of their computational efficiencies and statistical errors when calculating κ_ℓ . We perform calculations on both bulk-Si and Si with varying concentrations of vacancies using the Stillinger–Weber (SW) potential [17].

2. Background

In order to calculate κ_ℓ with the GK and HNEMD methods, calculation of the heat current is essential. The heat current \mathbf{J} is a vector quantity that characterizes the change with time of the spatial average of the local energy and is given as

$$\mathbf{J} = \frac{1}{\Omega} \frac{d}{dt} \sum_i \mathbf{r}_i(t) \epsilon_i(t), \quad (1)$$

where Ω is the volume of the system and ϵ_i and \mathbf{r}_i are the total energy [2] and coordinate vector of atom i .

2.1. The GK method

The GK method [18, 19] is an equilibrium MDs approach that relates \mathbf{J} to κ_ℓ via the fluctuation–dissipation theorem,

$$\kappa_\ell = \frac{1}{k_B VT^2} \int \langle \mathbf{J}(0) \otimes \mathbf{J}(t) \rangle dt, \quad (2)$$

where, k_B is the Boltzmann constant, V the volume of the system, T the temperature and $\langle \mathbf{J}(0) \otimes \mathbf{J}(t) \rangle$ the heat current auto-correlation function (HCACF). In general, κ_ℓ is a second-order tensor but in a material with cubic symmetry it reduces to a scalar. The discretized form of the HCACF, equation (2), is given as

$$\kappa_\ell = \frac{\Delta t}{k_B VT^2} \sum_{m=1}^M \sum_{n=1}^{N-m} \frac{\mathbf{J}(m+n)\mathbf{J}(n)}{N-m}, \quad (3)$$

where Δt is the length of a single MD timestep and M determines the length of the correlation time given by $M\Delta t$ over which the integration is done. $\mathbf{J}(m+n)$ is the heat current at MD timestep $m+n$. It should be noted that the number of integration steps M must be less than the total number of simulation steps N .

Two potential errors can arise while calculating κ_ℓ via equation (3). First of all, the correlation function $\langle \mathbf{J}(0) \otimes \mathbf{J}(t) \rangle$ is usually calculated as a time-average from the data of a single simulation and using a finite averaging time $\tau_N = N\Delta t$ in equation (3) which leads to an averaging error. Secondly, there is a truncation error related to M . Ideally M should be so that the HCACF has decayed to zero [2]. Too small M would underestimate κ_ℓ and a too large value would lead to large statistical errors as the heat current is dominated by noise after a certain correlation time [20].

2.2. Homogeneous non-equilibrium MDs

In HNEMD a fictitious force field is used to mimic the effect of a thermal gradient. It uses the linear response theory to calculate the transport coefficients in which the long-time ensemble average of the heat current vector, $\langle \mathbf{J}(t) \rangle$, for the resulting non-equilibrium system can be shown to be proportional to the external force field, \mathbf{F}_e , when the latter is sufficiently small [9, 21].

The detailed implementation of the HNEMD method for systems governed by three-body potentials can be found in [12]. The equation to consider is,

$$\frac{\langle \mathbf{J}(t) \rangle}{VT} = \left[\frac{1}{k_B VT^2} \int_0^\infty \langle \mathbf{J}(0) \otimes \mathbf{J}(t) \rangle dt \right] \mathbf{F}_e = \kappa_\ell \mathbf{F}_e. \quad (4)$$

It shows a linear relationship between the external perturbation field \mathbf{F}_e and the induced heat current $\mathbf{J}(t)$. The constant of proportionality (κ_ℓ) is the GK formula for the heat transport coefficient tensor, equation (2). In this way, the thermal conductivity can be obtained without explicitly calculating the auto-correlation functions. Hence, one can circumvent the problems related to the calculation and integration of autocorrelation functions associated with the GK method described above.

3. Results and discussion

We carried out all the simulations in silicon system on a $6 \times 6 \times 6$ supercell containing 1728 atoms and with a lattice parameter of 5.431 Å using the SW potential [17] and the LAMMPS package [22]. The choice of the parameters was based on previous finite size dependence studies done on silicon using MD techniques [2, 20, 23]. In each simulation, after the velocity initialization the system was equilibrated under zero pressure at 1000 K (NPT ensemble).

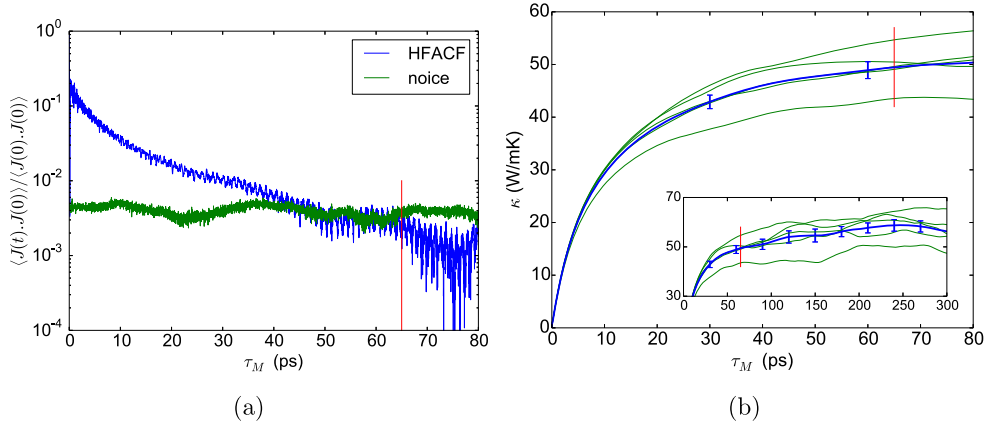


Figure 1. (a) Representative HCACF for Si (SW potential) as a function of $\tau_M = M\Delta t$, normalized to the value at $t = 0$ (Blue line). (b) Thermal conductivity of Si calculated by the direct integration of the HCACF, with the redline showing τ_c . The blue line depicts the averaged thermal conductivity over 5 independent simulations (green lines). Also shown in the inset is κ_ℓ calculated for the total correlation time of 300 ps and error bars can be seen growing rapidly after 65 ps (red line) because of the calculations being dominated by noise.

3.1. Bulk conductivity

From the GK method the thermal conductivity was obtained through equation (3). The HCACF was sampled at every timestep for better accuracy of the correlation integral. The simulations were then run in the NVE ensemble for the calculation and sampling of the HCACF. A time step of $\Delta t = 1.0$ fs was chosen to ensure long-time stability of the HCACF.

The averaging error can be minimized either by performing one simulation for a very large number of time steps or by carrying out multiple independent simulations for smaller time durations. We have applied the latter technique in which the simulations can be run in parallel and we collected a total of 60 ns of data comprising of 5 independent simulations of $N = 12$ ns (12×10^6 timesteps) each. These independent simulations vary only with respect to the random seed provided for generating the initial atomic velocities [2, 20]. The total correlation length for a single simulation was 300 ps (3×10^5 timesteps).

In order to minimize the truncation error, we employed the idea of a maximum significant correlation time (τ_c) [24] to determine an optimum M . Figure 1(a) shows the ensemble averaged HCACF together with the noise (green line) which is estimated as the root mean square of the heat current cross-correlation functions [20],

$$\zeta = \sqrt{\frac{\langle J_x(t)J_y(0) \rangle^2 + \langle J_y(t)J_z(0) \rangle^2 + \langle J_z(t)J_x(0) \rangle^2}{3}}. \quad (5)$$

τ_c is the time after which the noise crosses and becomes larger than the HCACF and is shown as a red line in figure 1(a). The HCACF can be seen to decay and at $\tau_M \equiv \tau_c \simeq 65$ ps (red line) the noise overtakes the HCACF.

Next, κ_ℓ was calculated by direct integration of the HCACF. Figure 1(b) shows the value of κ_ℓ versus the correlation time. The integration till $\tau_c = 65$ ps gives a value of 49.6 ± 1.5 W (m K) $^{-1}$. This value is in good agreement to the other GK calculations 53.3 ± 5.2 W (m K) $^{-1}$ [4, 24], lower than but consistent with 66 ± 16 W (m K) $^{-1}$ [2]. It is also slightly lower than 53 ± 3 W (m K) $^{-1}$ reported by Howell *et al* [20] because they

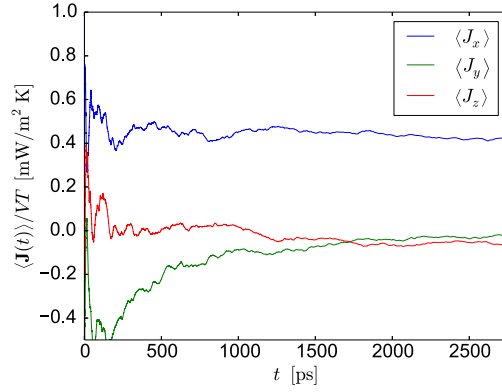


Figure 2. The running average of components of the heat current \mathbf{J} in the x , y and z directions for Si with $F_e = 8 \times 10^{-5} \text{ \AA}^{-1}$ applied in the x direction.

calculated κ_ℓ by integrating till ∞ an exponential function fitted to the values of κ_ℓ averaged over five independent samples. They mentioned that the contribution to the total value of κ_ℓ by correlation times greater than τ_c is $<5\%$. Recently, Jones *et al* [24] proved that the relative error in the estimate of κ_ℓ is bounded by the ratio of maximum significant correlation time (τ_c) and the total simulation time K as $2\sqrt{\tau_c/K}$, which in our case reduces to $\approx\sqrt{M/N}$. This limits the relative error to be less than 6.5%, which is consistent with our results.

From the HNEMD method the thermal conductivity was obtained through equation (4). A time-independent external perturbation field F_e was applied in the x direction. The calculations were carried out for a total of 22 F_e values ranging from 1×10^{-5} to $3 \times 10^{-4} (\text{ \AA}^{-1})$ at 1000 K for 5×10^6 time steps each of duration of 0.55 fs and running averages of the heat currents were collected for each simulation. Figure 2 shows the behavior of the running average of the heat current with the external perturbation field, $F_e = 8 \times 10^{-5} \text{ \AA}^{-1}$. As can be seen in the figure, the initial fluctuations of heat current are very high and they stabilize at ≈ 2000 ps. Consequently, we choose to cut off sampling $\langle \mathbf{J} \rangle$ at $t = 2750$ ps. This lead to a bulk thermal conductivity of $53.4 \text{ W (m K)}^{-1}$ at 1000 K, see figure 3(a). Cutting the sampling at $t = 2400$ ps lead to $\kappa_\ell = 52.6 \text{ W (m K)}^{-1}$, underlining that the results are well converged.

We have considered two methods for calculating κ_ℓ from $\langle \mathbf{J}(t) \rangle$. In the gradient method the slope of a least-squares fit of $\langle J_x(t) \rangle / VT$ versus F_e is identified as the thermal conductivity, equation (4). We assume that the intercept is zero. In the mean method κ_ℓ is calculated by averaging the κ_ℓ 's obtained from several individual runs with varying F_e . For bulk-Si, the values of thermal conductivity calculated by the gradient and mean methods are $\kappa_\ell = 53.4 \pm 1.9 \text{ W (m K)}^{-1}$ figure 3(a) and $53.2 \pm 6.7 \text{ W (m K)}^{-1}$ figure 3(b), respectively. The values are in good internal agreement the GK calculations as well as the earlier HNEMD calculations [12].

One observation is that the determination of the range where κ_ℓ depends linearly on F_e is important. For the bulk-Si runs, it can be seen in figure 3(a) that the values of κ_ℓ deviate strongly from a linear behavior for $F_e > 2 \times 10^{-5} \text{ \AA}^{-1}$. The other possible shortcoming of the HNEMD method is that it is inefficient for very small values of F_e . At very small values of F_e all the three components of \mathbf{J} are almost equal suggesting that the system is still in equilibrium. Due to this, the estimation of the ratio $\langle \mathbf{J}(t) \rangle / TF_e$ becomes very difficult, as $\langle J_x(t) \rangle$ approaches zero for these values. Hence, it is crucial to determine a range of F_e that is large enough to obtain reasonable values of $\langle J_x(t) \rangle / TF_e$ and small enough for the system to be

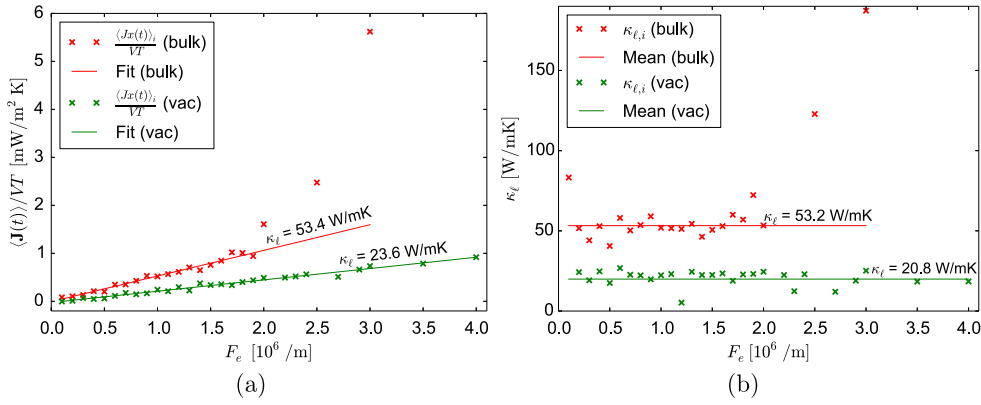


Figure 3. (a) Running average of heat current \mathbf{J} as a function of F_e in bulk (red) and defected Si with five randomly distributed vacancies (green). The thermal conductivity is obtained via the gradient method. (b) κ_ℓ as a function of F_e used to obtain the thermal conductivity via the mean method for both bulk and vacancy Si.

in the linear non-equilibrium range [12]. A fine scan over different values of F_e is required to correctly estimate κ_ℓ .

3.2. Influence of vacancies on κ_ℓ of Si

In order to compare the performance of GK and HNEMD methods in defected structures, we carried out κ_ℓ calculations for 1 to 10 (0.06–0.57 atomic %) randomly distributed vacancies in the $6 \times 6 \times 6$ Si supercell (1728 atoms in bulk) at 1000 K. To minimize the interaction of vacancies among themselves, the vacancies were distributed in such a manner that no two vacancies were within the second nearest neighbor distance of one another.

Although, both the methods agree well in terms of thermal conductivity predictions for defect structures, figure 4(a), we would like to point out that for the defected structures the calculation of κ_ℓ becomes easier with HNEMD method. This is illustrated as follows. In section 3.1 we saw that one of the shortcomings of the HNEMD method is the difficulty in determining the linear range of $\langle J_x(t) \rangle / VT$ versus F_e . However, in our calculations for defected Si, we observed that as the vacancy concentration increases $\langle J_x(t) \rangle / VT$ versus F_e remains linear for higher and higher values of F_e . This can be observed in figure 3(a) which shows a comparison of the linear regimes in bulk and defected Si. It can be clearly seen in figure 3(a) that one has to do a fine scan over F_e values in case of bulk to find out the exact linear range. The relation between $\langle J_x(t) \rangle / VT$ and F_e becomes nonlinear already around $F_e = 2 \times 10^{-5} \text{ \AA}^{-1}$, whereas in case of defect structure the plot is still linear for values as high as $40 \times 10^{-5} \text{ \AA}^{-1}$. This behavior is also illustrated in figure 3(b) where, for bulk the κ_ℓ values deviate for higher F_e whereas for the defected structure they are stable. Hence, in case of defected structures one can obtain the linear range and therefore κ_ℓ using fewer values of F_e thereby reducing the computational cost.

We found an inverse power-law like decay of κ_ℓ against the vacancy concentration, c , for both GK and HNEMD methods confirming a good agreement between the two methods, figure 4(a). Following the discussion above, we performed κ_ℓ calculations at 700 K using only HNEMD method. An inverse power-law decay for κ_ℓ versus c was also observed at 700 K, as shown in figure 4(b). We also tried to fit exponential functions to κ_ℓ 's but the standard deviation for the fit values was orders of magnitude higher than the power-law fit.

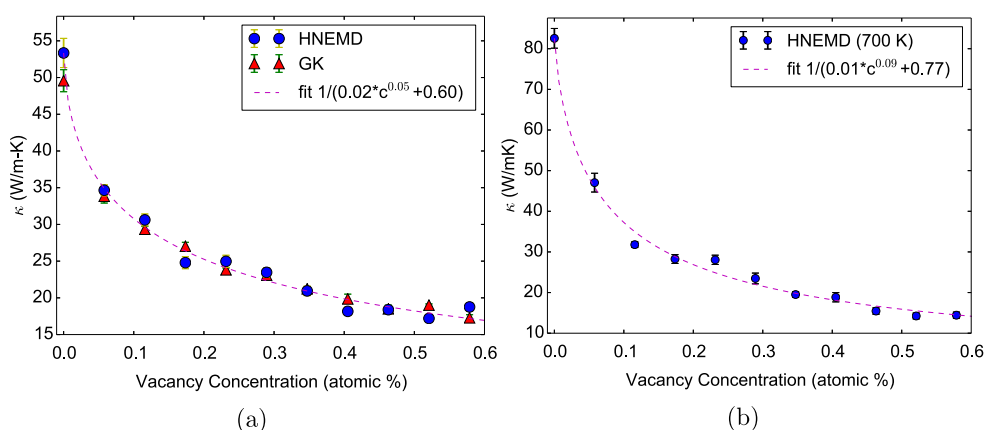


Figure 4. (a) Comparison of GK and HNEMD methods with regards to κ_{ℓ} versus vacancy concentration for Si at 1000 K. (b) κ_{ℓ} versus vacancy concentration for Si at 700 K.

Hence we can establish that the thermal conductivity falls according to inverse power-law with increasing vacancy concentration in crystalline Si. Our results agree well the literature [14, 16, 25].

4. Conclusions

We have done a detailed study of the GK and HNEMD methods for calculating κ_{ℓ} in bulk and defected Si and highlighted the advantages and disadvantages of each method. We have discussed the underlying parameters of the two methods and shown that by a judicious choice both the methods performed equally well for κ_{ℓ} calculations in bulk Si. The GK method in the above fashion produces very accurate values of thermal conductivity within statistical uncertainties. With the GK method the entire lattice thermal conductivity tensor can be calculated from one simulation, unlike the HNEMD method which necessitates several simulations in each direction to achieve the same. At the same time the GK method can suffer from averaging and truncation errors which makes it more cumbersome than the HNEMD method. Both the GK and the HNEMD method require several independent simulations to get a κ_{ℓ} with a low uncertainty. These simulations in the respective methods are not inter-dependent and can be run in parallel. The HNEMD method has an advantage over the GK method as it generates lesser statistical errors and reduces the necessary computation time by combining the elements of both equilibrium and non-equilibrium MD simulations. Specially in case of defect structures HNEMD can be advantageous.

Acknowledgments

We acknowledge Dr Mandadapu and Prof Dr Papadopoulos for the helpful discussions and the HNEMD code, and the European Union's Horizon 2020 Research and Innovation Programme, grant number 645776 (ALMA).

References

- [1] Cahill D G, Ford W K, Goodson K E, Mahan G D, Majumdar A, Maris H J, Merlin R and Phillpot S R 2003 *J. Appl. Phys.* **93** 793–818
- [2] Schelling P K, Phillpot S R and Keblinski P 2002 *Phys. Rev. B* **65** 144306
- [3] Müller-Plathe F 1997 *J. Chem. Phys.* **106** 6082–5
- [4] McGaughey A J and Kaviani M 2006 *Adv. Heat Transfer* **39** 169–255
- [5] Stackhouse S and Stixrude L 2010 *Rev. Mineral. Geochem.* **71** 253–69
- [6] Turney J, Landry E, McGaughey A and Amon C 2009 *Phys. Rev. B* **79** 064301
- [7] Sellan D P, Landry E S, Turney J, McGaughey A J and Amon C H 2010 *Phys. Rev. B* **81** 214305
- [8] McQuarrie D A 2000 *Statistical Mechanics* (Sausalito, CA: University Science Books) 12 641
- [9] Evans D J 1982 *Phys. Lett. A* **91** 457–60
- [10] Berber S, Kwon Y K and Tománek D 2000 *Phys. Rev. Lett.* **84** 4613
- [11] Lukes J R and Zhong H 2007 *J. Heat Transfer* **129** 705–16
- [12] Mandadapu K K, Jones R E and Papadopoulos P 2009 *J. Chem. Phys.* **130** 204106
- [13] Klemens P and Pedraza D 1994 *Carbon* **32** 735–41
- [14] Wang T, Madsen G K H and Hartmaier A 2014 *Modelling Simul. Mater. Sci. Eng.* **22** 035011
- [15] Katcho N, Carrete J, Li W and Mingo N 2014 *Phys. Rev. B* **90** 094117
- [16] Lee Y, Lee S and Hwang G S 2011 *Phys. Rev. B* **83** 125202
- [17] Stillinger F H and Weber T A 1985 *Phys. Rev. B* **31** 5262
- [18] Green M S 1954 *J. Chem. Phys.* **22** 398–413
- [19] Kubo R 1957 *J. Phys. Soc. Japan* **12** 570–86
- [20] Howell P 2012 *J. Chem. Phys.* **137** 224111
- [21] Evans D J and Holian B L 1985 *J. Chem. Phys.* **83** 4069–74
- [22] Plimpton S 1995 *J. Comput. Phys.* **117** 1–19
- [23] Che J, Çağın T, Deng W and Goddard W A III 2000 *J. Chem. Phys.* **113** 6888–900
- [24] Jones R E and Mandadapu K K 2012 *J. Chem. Phys.* **136** 154102
- [25] Shahraki M G and Zeinali Z 2015 *J. Phys. Chem. Solids* **85** 233–8